Poly(acrylic acid)-Lined Nanotubes of Poly(butyl methacrylate)-*block*-poly(2-cinnamoyloxyethyl methacrylate)

Xiaohu Yan, Futian Liu, Zhao Li, and Guojun Liu*

Department of Chemistry, University of Calgary, 2500 University Dr., NW, Calgary, Alberta, Canada T2N 1N4

Received July 23, 2001; Revised Manuscript Received September 30, 2001

ABSTRACT: Two triblock copolymers of the poly(butyl methacrylate)-*block*-poly(2-cinnamoyloxyethyl methacrylate)-*block*-poly(*tert*-butyl acrylate) or PBMA-*b*-PCEMA-*b*-P*t*BA family were synthesized and characterized. The triblocks had PCEMA to P*t*BA volume ratios ≥1.3 and PBMA volume fractions ≥0.56. Their bulk morphologies consisted of cylindrical domains with P*t*BA cores and PCEMA shells dispersed in the PBMA matrix. Nanofibers of PBMA-*b*-PCEMA-*b*-P*t*BA were obtained after cross-linking PCEMA photochemically and separating the cross-linked cylinders from dissolved PBMA chains. PBMA-*b*-PCEMA nanotubes with PAA-lined channels were obtained after *tert*-butyl group removal from the P*t*BA cores by selective hydrolysis.

I. Introduction

Block copolymers self-assemble in bulk forming various intricate nanometer-sized block segregation patterns.[1,2] Block-segregated solids of diblock copolymers have been processed chemically in the past to yield nanofibers,[3−6] nanospheres,[7] nanochannels in thin films,[8,9] inorganic nanoparticles in polymer matrices,[10−13] and lithographic masks with nanometer-sized patterns.[14] Linear triblocks $A_nB_mC_l$ are far richer in block segregation patterns than diblocks, as the patterns are governed not only by the volume fractions of the different blocks, as in the diblock case, but also by the linking sequence of the blocks and the relative strength of block−block interactions. For example, cylinders formed by the minority block of a diblock can exist only as hexagonally packed arrays dispersed in the matrix of the majority block. Cylinders formed by the minority block of a linear triblock can, however, be encapsulated in cylinders or lamellae formed by another block or at the interface between two lamellae.[15−18] They can also form equally spaced circular loops around cylinders of another block or be on the surfaces of cylinders of another block in a parallel or helical fashion.[15−18] Despite the richness of triblock self-assembly, there have been only a few reports[19−21] of nanostructure preparation from block-segregated triblock solids. Here we report on the preparation of poly(acrylic acid)- or PAA-lined nanotubes from two triblocks of the poly(butyl methacrylate)-*block*-poly(2-cinnamoyloxyethyl methacrylate)-*block*-poly(*tert*-butyl acrylate) or PBMA-*b*-PCEMA-*b*-P*t*BA family:

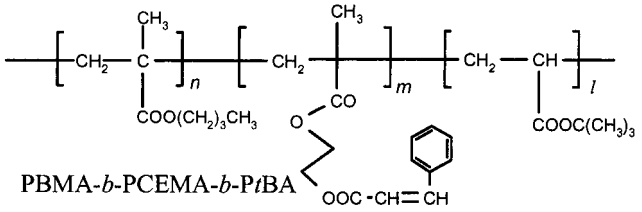

PBMA-*b*-PCEMA-*b*-P*t*BA

where *n*, *m*, and *l* are 1270, 190, and 270 for sample 1 and 630, 180, 210 for sample 2, respectively.

The preparation involved first the self-assembly of the blocks in thin films into concentric PCEMA and P*t*BA cylinders dispersed in the PBMA matrix (A → B of Scheme 1). The cylindrical structures were then locked in by photo-cross-linking the PCEMA shells (B → C). Dissolving the films in THF yielded individual nanofibers with PBMA coronas, PCEMA middle layers, and P*t*BA cores (C → D). Nanotubes with PAA-lined cores were obtained after cleaving the *tert*-butyl groups from P*t*BA (D → E).

II. Experimental Section

Polymer Synthesis. Although there has been no report of PBMA-*b*-P(HEMA-TMS)-*b*-P*t*BA preparation by anionic polymerization, where HEMA-TMS denotes 2-trimethylsilylethyl methacrylate, anionic polymerization has been used previously to prepare P(HEMA-TMS)-*b*-P*t*BA by us[22] and random copolymers of BMA and methyl methacrylate by Haddleton et al.[23] For this, we will not dwell on monomer preparation and purification procedures. PBMA-*b*-P(HEMA-TMS)-*b*-P*t*BA was prepared by sequential living anionic polymerization in 500 mL of THF at −78 °C using the standard vacuum line technique.[24] Lithium chloride, ∼0.1 g, was used to decrease the polydispersity of the resultant polymers.[25] To prepare polymer 1, the initiator, 1,1-diphenyl-3-methylpentyllithium, was produced in THF from reacting *sec*-butyllithium (0.06 mL of 1.3 M solution in cyclohexane or 80 μmol) and an excess amount of 1,1-diphenylethylene (0.022 mL or 120 μmol). BMA (12.7 mL, 11.4 g, or 80 mmol), HEMA-TMS (3.5 mL, 3.2 g, or 16 mmol), and *t*BA (2.3 mL, 2.1 g, or 16 mmol) were each polymerized for 3 h. The polymerization was terminated by methanol. Stirring the triblock in THF/methanol (v/v = 75/25) overnight hydrolyzed the TMS groups to yield PBMA-*b*-PHEMA-*b*-P*t*BA, where PHEMA denotes poly(2-hydroxylethyl methacrylate). The polymer solution was then concentrated under reduced pressure, and the copolymer was precipitated on ice. The PHEMA block of the copolymer was converted to PCEMA from reacting with cinnamoyl chloride following conditions used previously.[26]

Polymer Characterization. Gel permeation chromatography (GPC) analysis of PBMA-*b*-PCEMA-*b*-P*t*BA was performed using THF as the eluant. The Waters HT-4 column used was calibrated using poly(methyl methacrylate) standards. The BMA to CEMA and to *t*BA ratios, *n*/*m*/*l*, were determined using ^{1}H NMR. The difference, Δn_r, between the refractive index of a polymer solution and that of chloroform, the solvent, was determined using a differential refractometer (Precision Instruments Co.) with light that had passed a bandpass filter centered around 633 nm. The absolute weight-

10.1021/ma0112927 CCC: $20.00
Published on Web 11/17/2001

Scheme 1

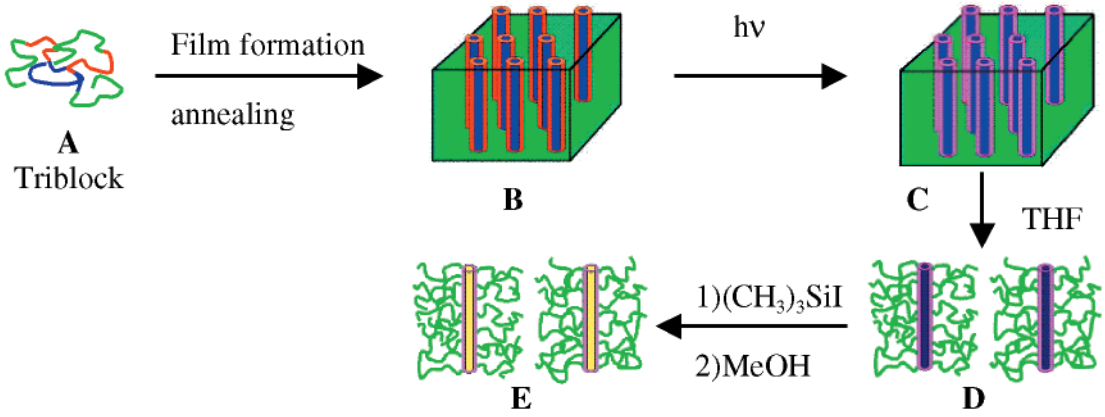

Table 1. Characteristics of the Triblock Copolymers

sample	dn_r/dc (mL/g)	$10^{-4} \times$ LS $\bar{M}_w$ (g/mol)	GPC $\bar{M}_w/\bar{M}_n$	NMR $n/m/l$	n	m	l	V_{BMA}	V_{CEMA}
1	0.057	26.4	1.27	1.00/0.15/0.21	1270	190	270	0.70	0.17
2	0.062	16.4	1.14	1.00/0.29/0.33	630	180	210	0.56	0.26

average molar masses were measured in chloroform using a light scattering instrument (Brookhaven model 9025) equipped with a 632 nm He−Ne laser.

Solid Sample Preparation. Bulk films, ~0.2 mm thick, were obtained from evaporating slowly over several days a concentrated solution, ~20 wt %, of a triblock in toluene in closed polyethylene capsules or vials. The films were then annealed at 45 and 65 °C each for 1 day and then at 105 °C for 5 days. A small piece of the film was used to check the morphology. For density measurement, a method described previously[8a] was used. The density thus measured of a PBMA sample with a GPC molar mass of ~60 000 g/mol was 1.08 g/cm^3.

PCEMA Cross-Linking and *tert*-Butyl Group Removal. The PCEMA domains of the annealed triblock films were cross-linked with a focused UV beam that had passed a 310 nm cutoff filter from a 500 W mercury lamp. The progress of the cross-linking was followed by FTIR spectrometry.

Nanofibers were obtained after stirring the irradiated films in THF overnight. The THF solutions were then filtered through glass wool and added into methanol to precipitate the nanofibers. The dried nanofibers were redispersed in dichloromethane freshly distilled over CaH_2. Trimethylsilyl iodide, at 2 molar equivalents to the *tert*-butyl groups, was added, and the mixture was stirred for 1 h before methanol containing 2% water was added to decompose the excess trimethylsilyl iodide and the trimethylsilyl acrylate groups formed. The resultant PAA-lined nanotubes were purified from precipitation into methanol containing ice.

Iron Oxide Loading. A literature method was followed to load the cores of the nanochannels supposedly with γ-Fe_2O_3.[27] After dispersing or dissolving the nanotubes in THF, ferrous chloride, at 10 molar equivalents to the acrylic acid groups, was added. The mixture was stirred for 24 h or longer before it was added into methanol/water (50/50 in v/v) to precipitate out the nanotubes. This procedure of nanotube redissolution in THF and reprecipitation into methanol/water was repeatedly four times to remove Fe^{2+} external to the nanotubes. After the final precipitation, the tubes were dissolved in THF with 2 vol % water, and the solution pH was increased to 10 with 0.10 M NaOH. All operations before this were executed under N_2 atmosphere, and all solvents used were bubbled with N_2. Two hours after NaOH addition, excess hydrogen peroxide was added to the nanotube dispersion, and the mixture was stirred for 3 h to oxidize ferrous oxide inside the nanotubes. The Fe_2O_3-loaded nanotubes were purified by precipitation into the methanol/water (50/50) again to remove the excess sodium hydroxide and hydrogen peroxide. The amount of Fe_2O_3 loaded into each gram of nanotubes was determined from thermogravimetric analysis following a literature method.[28]

TEM Studies. To check the morphologies of sample 1 and 2 solids, sections, ~50 nm thick, were obtained from ultramicrotoming. The samples were then placed in a vial containing osmium tetraoxide (Aldrich) vapor for 4 h to stain the double bonds. Transmission electron microscopy (TEM) images were obtained using a Hitachi H-7000 instrument operated at 75 kV. Nanotube specimens were obtained from aspirating a THF solution of the tubes on carbon-coated copper grids using a home-built device.[29] The Fe_2O_3-impregnated nanotubes were mixed with a polystyrene standard (Pressure Chem. Co., MW = 2500, polydispersity = 1.09) at the mass ratio of 1:20 in THF before spraying. Polystyrene was used as a binder to minimize nanotube loss in the TEM magnets.[30]

III. Results and Discussion

In this section, we will first show the characterization results for the triblocks and then demonstrate the formation of cylindrical domains with PCEMA shells and P*t*BA cores dispersed in the PBMA matrix. Microscopic images will be presented in the last part to show the preparation of PAA-lined nanotubes.

Polymer Synthesis and Characterization. Our success in preparing the triblocks was confirmed from ^{1}H NMR analyses of the end products. From the relative intensities of peaks of different blocks we obtained $n/m/l$ = 1.00/0.15/0.21, which agree reasonably well with 1000/200/200, where 1000, 200, and 200 are the targeted n, m, and l numbers. The $n/m/l$ values for sample 2 from ^{1}H NMR are 1.00/0.29/0.33, which agree well with the targeted ratios of 600/200/200.

The variation in refractive index differences, Δn_r, of PBMA-*b*-PCEMA-*b*-P*t*BA solutions and chloroform was plotted in the form of $\Delta n_r/c$ vs c for each sample.[31] Extrapolating the $\Delta n_r/c$ data to zero concentration yielded the refractive index increments dn_r/dc of 0.057 and 0.062 for samples 1 and 2, respectively (Table 1). The refractive index, n_r, of chloroform at 20 °C is 1.446, that of PBMA is 1.483,[32] and that of poly(butyl acrylate) is 1.466,[32] which should be close to that of P*t*BA. In toluene with a refractive index of 1.4961,[32] we measured the dn_r/dc value of 0.0935 mL/g for PCEMA. Thus, PCEMA should have the highest n_r of the three samples, and an increase in dn_r/dc with increasing PCEMA content from sample 1 to 2 was reasonable.

The weight-average molar masses of the triblocks were determined by light scattering using the Zimm

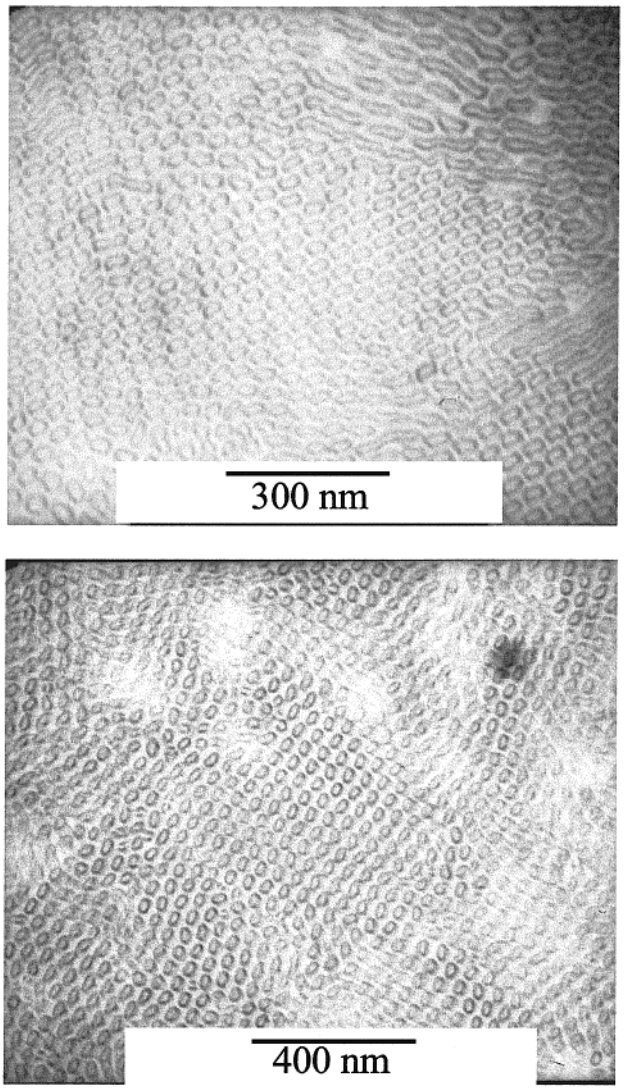

Figure 1. TEM images of 50 nm sections of sample 1 (a, top) and sample 2 (b, bottom). The samples were stained with OsO_4 vapor.

method, and the results are shown in Table 1. The molar masses were apparent, because the dn_r/dc values for the three blocks were different and each block had a molar mass distribution.[31] While we do not know how to correct for the sample heterogeneity effect to obtain the true molar masses, the correction factor should be close to 1 as the dn_r/dc values in $CHCl_3$ should be positive for all the three blocks. Combining the light scattering and NMR results, we obtained the weight-average *n*, *m*, and *l* values for the triblocks as listed in Table 1. The determined apparent *n*, *m*, and *l* values coincided quite well with the targeted values.

GPC analysis gave a lower polydispersity for the sample with a lower molar mass. The GPC peak for the higher molar mass sample exhibited a slight shoulder on the lower molar mass side. This could have been due to partial chain termination by impurities present in the TMS−HEMA and *t*BA monomers. Partial chain termination manifests itself more predominantly at a lower initiator concentration used to make a higher molar mass sample.

Morphologies of the Triblocks. Shown in Figure 1a,b are TEM images of thin sections of samples 1 and 2 annealed at 105 °C for 5 days. Hexagonally packed ellipses with dark shells and light cores dominate in the two pictures. At places short stems are seen attached to the ellipses. Also, strips with light cores are seen in Figure 1a. Since the thin sections for TEM studies were stained with OsO_4, only the PCEMA domains should appear dark in the images. The above observations suggest that PCEMA and P*t*BA formed hexagonally packed concentric cylinders dispersed in the PBMA matrix. The projections of the cylinders are elliptic in Figure 1a,b, because the cylinders were deformed along the microtoming direction and could lie also off the normal direction of the images.

Table 2. Dimensions of the Core−Shell Cylinder Morphologies

sample	*L*/nm	d_c/nm	l_s/nm
1	45	17	8
2	46	20	6

Although both PBMA and P*t*BA appeared light in the TEM images, only PBMA could have made up the matrix due to its large volume fraction. On the basis of the densities of 1.08, 1.25, and 1.02 g/mL for PBMA, PCEMA,[8a] and P*t*BA,[8a] the volume fractions of PBMA are 0.70 and 0.56 for samples 1 and 2, respectively. Also listed in Table 1 are the volume fractions of PCEMA. The volume fractions of P*t*BA can be calculated from the fact that the volume fractions of the three components add to 100%. Because of sample deformation during microtoming, it was difficult to determine the cylinder core diameters, d_c, and shell thickness, l_s, accurately from Figure 1a,b. We have thus followed the approach of Breiner et al.[15a] to calculate d_c and l_s from the volume fractions of different blocks and the inter-cylinder distances, *L*, which were estimated more accurately from the TEM images. These values are shown in Table 2.

A close examination of Figure 1a,b reveals no abnormality in the ring patterns of PCEMA. Also seen in Figure 1a are some light P*t*BA strips surrounded by uniform PCEMA layers. These suggest that the cylinders formed were of the core−shell type rather than the cylinder-on-cylinder or cylinder-at-cylinder morphologies seen by Breiner et al.[15a]

Nanostructructures of Samples 1 and 2. Polymer films with block-segregation patterns shown in Figure 1a,b were then irradiated with UV light to cross-link the PCEMA shells. The cross-linked cylindrical domains separated from one another in THF yielding nanofiber dispersions that were stable for days. The nanofiber dispersions or solutions could then be treated with trimethylsilyl iodide to hydrolyze the *tert*-butyl groups selectively to yield nanotubes with PAA-lined channels in the centers. The photo-cross-linking[26] and *tert*-butyl cleavage[22] reactions have been used extensively in our group in the past, and the selectivity of the hydrolysis conditions to the *tert*-butyl esters over other esters has been demonstrated as well.

Illustrated in Figure 2a is a TEM image of the PAA-lined nanotubes of sample 2 sprayed on a carbon-coated copper grid from THF. Such tubes can be tens of micrometers long, and each seems to have a layered structure with an irregularly sized darker inner part surrounded by a fuzzy outer layer. The diameter of the inner part at fatter sections reached ∼44 nm but was only ∼26 nm at the site marked with an arrow. The darker inner part must consist of PCEMA-*b*-PAA, and the fuzzy outer layer consists of PBMA. This assignment is in agreement with the fact that only PCEMA was stained, and the diameter of the original PCEMA-*b*-

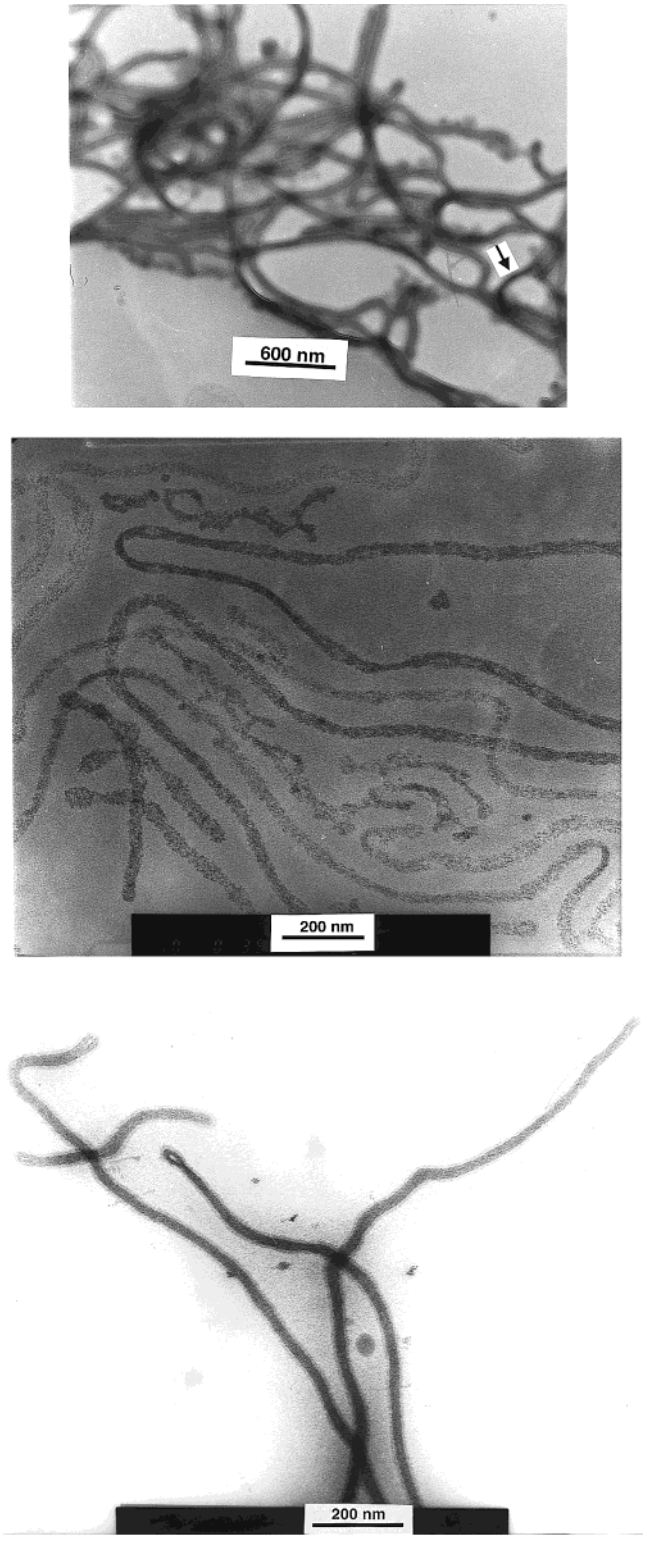

Figure 2. TEM images of sample 2 nanotubes (a, top), Fe_2O_3-impregnated nanotubes before OsO_4 staining (b, middle), and Fe_2O_3-impregnated nanotubes after OsO_4 staining (c, bottom).

P*t*BA cylinders in Figure 2a was ~32 nm (20 + 6 + 6 = 32, Table 2). The size of the inner part varied along the length of a nanotube probably because of nonuniform shrinking of the tube during solvent evaporation after sample spraying. A diameter larger than 32 nm could be accounted for by the retention of a swollen state by the tube due to fast THF evaporation. Thin sections could be obtained from slow solvent evaporation, which results in more nanotube shrinking. When completely shrunk, a section may have a diameter less than 32 nm because *tert*-butyl groups have been removed from the original P*t*BA core.

The fact that PAA made up the cores of the tubes could be concluded from several observations. First, we performed ^1H NMR analysis of sample 1 and 2 nanofibers. Only signals from PBMA were observed, despite the solubility of P*t*BA and uncrossed PCEMA chains in $CDCl_3$. This absence of P*t*BA signals could be due to the low mobility of the P*t*BA chains, which would result if the chains were in the cores. Second, the nanotubes dispersed readily in THF or CH_2Cl_2, which does not solubilize PAA. Third, we were able to load Fe_2O_3 into the cores. Shown in Figure 2b is a TEM image of such fibers sprayed on a carbon-coated copper grid. Since the sample was not stained, the visible part must have consisted of Fe_2O_3. The diameter of the Fe_2O_3-impregnated portion is always less than ~20 nm, which is the diameter of the P*t*BA cores shown in Figure 1b. Figure 2c shows a picture taken after OsO_4 staining of the Fe_2O_3-impregnated nanotubes. The encapsulating PCEMA layer is now visible, confirming Fe_2O_3 impregnation inside the PAA cores unambiguously. This production of Fe_2O_3 in the cores would also explain the stability of the tube dispersion for tens of hours in THF or other organic solvents that solubilize PBMA.

Similar results were obtained for sample 1. The results are not presented to avoid redundancy.

Fe_2O_3 Loading. The ferrous ions Fe^{2+} entered the PAA-lined nanochannels probably partially due to ion exchange with the protons of the acrylic acid groups but mostly due to their affinity for a more hydrophilic environment. Because of the favorable interaction between PAA chains and water, the water concentration in the nanochannels was probably much higher than its bulk concentration of 2%. Thus, Fe^{2+} would be concentrated in the nanochannels. As a result, the final Fe_2O_3 loading, 0.64 g per gram of nanotubes, was much higher than the theoretical value of 0.05 g obtained from assuming the binding of each Fe^{2+} by two carboxyl groups. The Fe_2O_3-impregnated tubes turned red and gave electron diffraction data that were reasonable for γ-Fe_2O_3. Because of the closeness of the crystal plane distances for Fe_2O_3 of other crystalline forms, we could not conclude unambiguously that the particles were γ-Fe_2O_3 despite the fact that the Fe_2O_3-impregnated tubes were attracted weakly by a magnet. We expect the Fe_2O_3 particles to be superparamagentic and to render many interesting properties to their encapsulating nanotubes such as their alignment in magnetic fields as demonstrated for PS-*b*-PCEMA-*b*-PAA/ Fe_2O_3 hybrid nanofibers.[33]

IV. Conclusion

We have synthesized and characterized two triblock copolymers of the PBMA-*b*-PCEMA-*b*-P*t*BA family. Both of the triblocks formed hexagonally packed cylindrical domains with PCEMA shells and P*t*BA cores dispersed in the PBMA matrix. Triblock nanofibers were prepared after cross-linking the PCEMA shells with UV light and separating the cross-linked cylindrical domains from the dissolved PBMA chains. The nanofibers must have consisted of PBMA coronas, PCEMA shells, and P*t*BA cores, because only the PBMA proton peaks were seen by NMR in $CDCl_3$. PAA-lined PBMA-*b*-PCEMA nanotubes were produced after the selective hydrolysis of

tert-butyl of P*t*BA. The location of PAA inside the cores was demonstrated by the production of Fe_2O_3 there.

Acknowledgment. We thank the NSERC of Canada for sponsoring this research financially. G. Liu also thanks the NSF of China for a distinguished young investigator award.

References and Notes

(1) Hasegawa, H.; Hashimoto, T. In *Comprehensive Polymer Science, Second Supplement*; Allen, G., Aggarwal, S. L., Russo, S., Eds.; Pergamon Press: London, 1996; pp 497−539.
(2) Bates, F. S.; Fredrickson, G. H. *Phys. Today* **1999** (Feb), 32.
(3) (a) Liu, G. J.; Ding, J.; Qiao, L.; Guo, A.; Gleeson, J. T.; Dymov, B.; Hashimoto, T.; Saijo, K. *Chem. Eur. J.* **1999**, *5*, 2740. (b) Liu, G. J.; Qiao, L.; Guo, A. *Macromolecules* **1996**, *29*, 5508−5510.
(4) Massey, J.; Power, K. N.; Manners, I. Winnik, M. A. *J. Am. Chem. Soc.* **1998**, *120*, 9533.
(5) Won, Y.-Y.; Davis, H. T.; Bates, F. S. *Science* **1999**, *283*, 960.
(6) Zhang, L.; Eisenberg, A. *Science* **1995**, *268*, 1728.
(7) Ishizu, K.; Fukutomi, T. *J. Polym Sci., Part C: Polym Lett.* **1988**, *26*, 281.
(8) (a) Liu, G. J.; Ding, J.; Hashimoto, T.; Saijo, K.; Winnik, F. M.; Nigam, S. *Chem. Mater.* **1999**, *11*, 2233. (b) Liu, G. J.; Ding, J.; Guo, A.; Herfort, M.; Bazett-Jones, D. *Macromolecules* **1997**, *30*, 1851.
(9) Lee, J.-S.; Hirao, A.; Nakahama, S. *Macromolecules* **1989**, *22*, 2602.
(10) Boontongkong, Y.; Cohen, R. E.; Rubner, M. F. *Chem. Mater.* **2000**, *12*, 1628.
(11) Fink, Y.; Urbas, A. M.; Bawendi, G. G.; Joannopoulos, J. D.; Thomas, E. L. *Lightwave Technol.* **1999**, *17*, 1963.
(12) Hashimoto, T.; Tsutsumi, K.; Funaki, Y. *Langmuir* **1997**, *13*, 6869.
(13) Templin, M.; Franck, A.; DuChesne, A.; Leist, H.; Zhang, Y. M.; Ulrich, R.; Schadler, V.; Wiesner, U. *Science* **1997**, *278*, 5344.
(14) Park, M.; Harrison, C.; Chaikin, P. M.; Register, R. A.; Adamson, D. H. *Science* **1997**, *276*, 1401.
(15) (a) Breiner, U.; Krappe, U.; Abetz, V.; Stadler, R. *Macromol. Chem. Phys.* **1997**, *198*, 1051. (b) Krappe, U.; Stadler, R.; Voigt-Martin, I. *Macromolecules* **1995**, *28*, 4558. (c) Auschra, C.; Stadler, R. *Macromolecules* **1993**, *26*, 2171. (d) Stadler, R.; Auschra, C.; Beckmann, J.; Krappe, U.; Voigt-Martin, I.; Leibler, L. *Macromolecules* **1995**, *28*, 3080.
(16) Gido, S. P.; Schwark, D. W.; Thomas, E. L. *Macromolecules* **1993**, *26*, 2636.
(17) Mogi, Y.; Mori, K.; Matsushita, Y.; Noda, I. *Macromolecules* **1992**, *25*, 5412.
(18) Matsushita, Y.; Tamura, M.; Noda, I. *Macromolecules* **1994**, *27*, 3680.
(19) Stewart, S.; Liu, G. J. *Angew. Chem., Int. Ed.* **2000**, *39*, 340−344.
(20) Saito, R.; Fujita, A.; Ichimuru, A.; Ishizu, K. *J. Polym. Sci., Part A: Polym. Chem.* **2000**, *38*, 2091.
(21) Erhardt, R.; Boker, A.; Zettl, H.; Kaya, H.; Pyckhout-Hintzen, W.; Krausch, G.; Abetz, V.; Muller, A. H. E. *Macromolecules* **2001**, *34*, 1069.
(22) Henselwood, F.; Liu, G. J. *Macromolecules* **1997**, *30*, 488.
(23) Haddleton, D. M.; Crossman, M. C.; Hunt, K. H.; Topping, C.; Waterson, C.; Suddaby, K. G. *Macromolecules* **1997**, *30*, 3992.
(24) Morton, M. *Anionic Polymerization: Principles and Practice*; Academic Press: New York, 1983.
(25) Creutz, S.; Teyssié, P.; Jérôme, R. *Macromolecules* **1997**, *30*, 6.
(26) Guo, A.; Tao, J.; Liu, G. J. *Macromolecules* **1996**, *29*, 2487.
(27) Ziolo, R. F.; Giannelis, E. P.; Weinstein, B. A.; O'Horo, M. P.; Ganguly, B. N.; Mehrotra, V.; Russell, M. W.; Huffman, D. R. *Science* **1992**, *257*, 219.
(28) Underhill, R. S.; Liu, G. J. *Chem. Mater.* **2000**, *12*, 3633.
(29) Ding, J.; Liu, G. J. *Macromolecules* **1999**, *32*, 8413.
(30) Underhill, R. S.; Liu, G. J. *Chem. Mater.* **2000**, *12*, 2082.
(31) Huglin, M. B. *Light Scattering from Polymer Solutions*; Academic Press: London, 1972.
(32) Brandrup, J.; Immergut, E. H. *Polymer Handbook*, 3rd ed.; Wiley & Sons: New York, 1989.
(33) Yan, X.; Liu, G. J.; Liu, F. *Angew. Chem., Int. Ed.* **2001**, *40*, 3593.

MA0112927